Check for updates

Pillar[5]arene-based multifunctional supramolecular hydrogel: multistimuli responsiveness, self-healing, fluorescence sensing, and conductivity†

Jin-Fa Chen, Qi Lin, [iD] Hong Yao, You-Ming Zhang [iD] and Tai-Bao Wei [iD] *

A novel pillar[5]arene-based multifunctional supramolecular hydrogel (**HG**) has been successfully constructed. The obtained supramolecular hydrogel shows excellent self-healing capacity. Meanwhile, this supramolecular hydrogel exhibited good multi-stimuli responsive behavior including thermal-responsiveness, pH-responsiveness, anion-responsiveness, and competitive agent-responsiveness. In addition, this hydrogel could effectively detect iron ions (Fe^{3+}) by fluorescence. The fluorescence spectra detection limit was 7.86×10^{-10} M, indicating the ultra-sensitivity of the hydrogel to Fe^{3+}. The thin film based on this hydrogel was also prepared, which was confirmed to be a convenient test kit for detecting Fe^{3+}. Furthermore, this supramolecular hydrogel (**HG**) is also an excellent conductive material.

Introduction

Hydrogels are 3D hydrophilic cross-linked soft materials with physical characteristics similar to soft biological tissues, and can hold a large amount of water *via* surface tension or capillary effect, making them increasingly important for widespread applications ranging from academic research to industrial fields.[1] In view of the types of driving forces for crosslinking, hydrogels can be divided into two major categories: chemical hydrogels and supramolecular hydrogels (physical hydrogel). Generally, chemical hydrogels are formed by permanent chemical crosslinks between the polymer chains *via* non-reversible covalent bonds.[2] Chemical hydrogels based on both natural and synthetic polymers have been of great interest for a wide range of biomedical applications from drug delivery to tissue engineering owing to their hydrophilic character and potential to be biocompatible.[3] However, such hydrogels are often brittle, at times opaque and without the ability to self-heal when the cross-linked network is broken, thus greatly limiting their application in various biomedical fields.[4]

Supramolecular hydrogels, which perfectly combine the advantages of chemical hydrogels with reversibility of supra-molecular interactions,[5] are a novel class of noncovalently

Key Laboratory of Eco-Environment-Related Polymer Materials, Ministry of Education of China, Key Laboratory of Polymer Materials of Gansu Province, College of Chemistry and Chemical Engineering, Northwest Normal University, Lanzhou, Gansu, 730070, P. R. China. E-mail: weitaibao@126.com; Fax: +86 9317973191; Tel: +86 9317973191

† Electronic supplementary information (ESI) available: Characterizations, ^{1}H NMR date and other materials. See DOI: 10.1039/c8qm00065d

cross-linked gel materials.[6] The supramolecular cross-linking by various noncovalent interactions such as hydrogen bonding, metal–ligand coordination, π–π stacking, host–guest recognition, and electrostatic interaction remarkably reduces the structural flexibility and alters the macroscopic performance, resulting in the formation of 3D cross-linked networks. In sharp contrast, such noncovalent hydrogels show not only the moderate mechanical properties gained from polymeric building blocks, but also show reversible gel–sol transition behavior in response to a wide variety of bio-related stimuli (*e.g.*, pH, redox agents, enzymes, bioactive molecules)[7] and processability inherent to the supramolecular cross-linking units, which can serve as either intelligent carriers for delivering versatile therapeutic agents (*e.g.*, drugs, genes, proteins)[8] or promising matrices for repairing and regenerating tissues and organs in the human body. Therefore, supra-molecular hydrogels have been attracting increasing attention from scientists.

Pillararenes,[9] a new class of macrocycles, are composed of hydroquinone units linked by methylene bridges at the *para* positions. Pillararenes have been garnering much attention due to their broad applications, such as fluorescent sensing,[10] biological imaging,[11] transmembrane transport,[12] gas adsorption[13] and so on.[14] Of course, pillararene-based supramolecular gels have also been constructed and prepared *via* various noncovalent inter-actions, especially host–guest interactions.[15] Many pillararene-based supramolecular gels have been reported, however, due to the poor solubility of pillararenes in aqueous media, most investigations of pillararene-based supramolecular gels have been conducted in organic media, which inhibit the application of pillararenes in soft materials. Therefore, to investigate and expand the applications of

This journal is © The Royal Society of Chemistry and the Chinese Chemical Society 2018

Mater. Chem. Front., 2018, **2**, 999–1003 | 999

pillararenes in water, preparation of the pillararene-based supra-molecular hydrogel is very necessary.[16]

Herein, following our success of pillar[5]arene-based supra-molecular chemistry,[17] a novel multifunctional fluorescent supramolecular hydrogel (**HG**) is successfully prepared by a functionalized pillar[5]arene-based self-assembly.[18] Compared with the chemical gels, this supramolecular hydrogel shows excellent self-healing capacity because of the dynamic self-assembly. It is worth to notice that the healing process in the supramolecular hydrogel is automatically without external treatment. Meanwhile, this supramolecular hydrogel also exhibited good thermal-responsiveness, pH-responsiveness, anion-responsiveness and competitive agent-responsiveness. In addition, this hydrogel could effectively detect iron ions (Fe^{3+}) by fluorescence. The fluorescence spectra detection limit was 7.86×10^{-10} M, indicating the ultra-sensitivity of the hydrogel to Fe^{3+}. More importantly, this supramolecular hydrogel (**HG**) is also an excellent conductive material.

Results and discussion

The gelator **BTAP5** is shown in Scheme 1 and the synthesis details are presented in Scheme S1 (ESI†). Gelator **BTAP5** and its intermediate have been characterized by ^{1}H NMR, ^{13}C NMR, and ESI mass spectrometry (Fig. S1–S9, ESI†).

Firstly, we established the self-assembly mode of **BTAP5** by ^{1}H NMR and 2D NOESY experiment. In the concentration dependent ^{1}H NMR spectrum of **BTAP5** (Fig. S10, ESI†), with the increasing amount of **BTAP5**, H_1, H_2 and H_3 signals of **BTAP5** showed a gradual downfield shift. Simultaneously, the $-CH_3$ (H_4) and $-CH_2$ (H_5) resonance signals showed obvious downfield shifts, respectively. These indicate that the n-butyl-trimethyl ammonium are partially included in the cavity of **BTAP5**, which was stabilized by C–H···O hydrogen bonding

interactions and C–H···π interactions. The assignment and correlation of the protons were further validated by the NOESY NMR spectrum of **BTAP5** (Fig. S11, ESI†). The NOESY spectrum of **BTAP5** shows cross peaks A and B representing the correlations between the signal of protons H_2 of aromatic protons and those of protons H_4 and H_5 of n-butyltrimethyl ammonium. Meanwhile, the cross peaks C and D also implied that the n-butyltrimethyl ammonium are included in the cavity of **BTAP5**. These results suggested that the aggregates of **BTAP5** changed from monomers into [c2]daisy chain dimers as the concentration increased (Scheme 1).

Secondly, the gelation properties of the synthesized gelator **BTAP5** were investigated. The novel supramolecular hydrogel was prepared by dissolving the monomers **BTAP5** in H_2O at 75 °C followed by cooling to room temperature, respectively. Upon increasing the concentration of the gelator, formed a hydrogel (**HG**) at a phase-transition temperature of approximately 28 °C for **BTAP5** at the concentration of 5 wt% (10 mg mL^{-1} = 1 wt%). It is noteworthy that the phase transfer temperature gradually increases with increasing the concentration of the gelator (Fig. S12, ESI†). Moreover, it is interesting to find that the high concentration **BTAP5** showed reversible glue–sol phase transitions upon heating and cooling, which could be reversibly achieved many times (Fig. 2). In order to learn the driving forces of the hydrogel formation process, the temperature dependences of **BTAP5** were investigated using the UV-Vis spectrum in H_2O solution. The absorbance of **BTAP5** (0.1 mM) slightly decreased with increasing temperature, implying the occurrence of intermolecular hydrogen bonding interactions because hydrogen bonds are temperature-dependent (Fig. S13, ESI†).[19] The X-ray peak (Fig. S14, ESI†) at $2\theta = 22.61°$ ($d = 3.93$ Å) confirms the π–π stacking interactions. Thus, the gelator **BTAP5** self-assembled to hydrogel **HG** through the hydrogen bonds and π–π stacking interactions. The morphological features of the hydrogel **HG** were studied using SEM and TEM (Fig. 1), and showed a loose nanosheet structure (Scheme 1).

According to SEM and TEM spectra, we can deduce two possible assembly processes. As shown in Fig. S15 (ESI†), we can easily find that the cavity of **BTAP5** forms 1:2 complexes with n-butyltrimethyl ammonium from the assembly process **1**. However, in the ESI-MS spectrum (Fig. S16, ESI†), we only found the 1:1 correlation peak between **DMP5** and **G'**, and no 1:2 correlation peak can be found. This phenomenon suggested that the nanosheet structure was formed due to stacking of [c2]daisy chain dimers. The [c2]daisy chain dimer
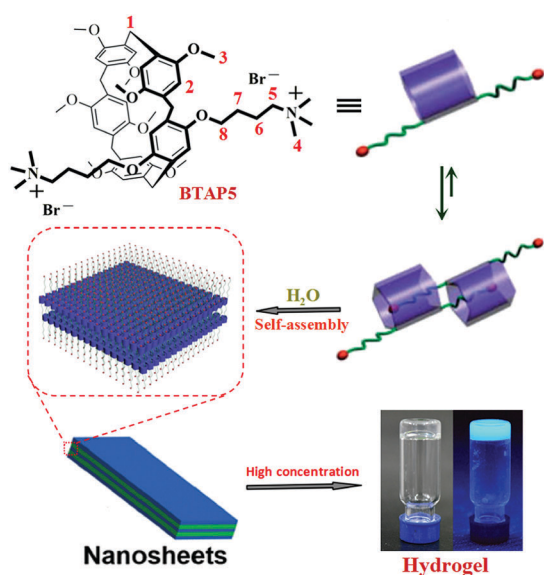
Scheme 1 Structure and proton designations of **BTAP5**, and further self-assembly to form a fluorescent supramolecular hydrogel.
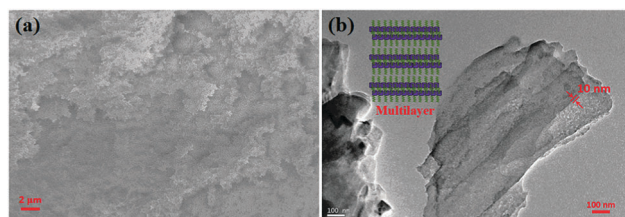

Fig. 1 SEM image (a) and TEM image (b) of gelator **BTAP5** self-assembly in water.
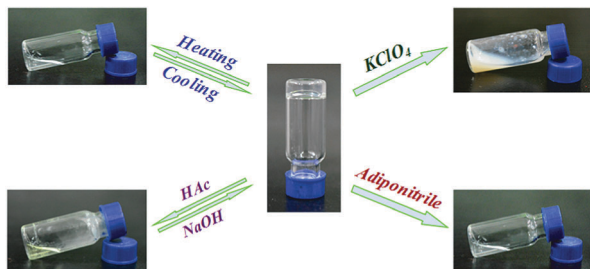
Fig. 2 The glue–sol transitions of the supramolecular hydrogel triggered by different stimuli.

Fig. 3 Photographs of the self-healing behavior of supramolecular hydrogel **HG**.

could be caused because the 1:1 complex was formed between the cavity of **BTAP5** and *n*-butyltrimethyl ammonium. In addition, the X-ray diffraction measurement also show a strong diffraction at 13.89° (Fig. S14, ESI†), which implied the thickness of the sheet-like structures. Hence, the calculated thickness of the sheet-like aggregates was 11.12 nm, which is larger than the extend length of the [c2]daisy chain dimer (Fig. S17, ESI†) and indicates that the nanosheets were multilayers.

The response to external stimuli was a significant property for smart hydrogels. Therefore, stimuli-responsive behaviors of the supramolecular hydrogel **HG** were investigated. As the acid has a strong proton-donating ability, the pH value of the solution has a strong effect on the formation of hydrogen bonds. Therefore, the supramolecular hydrogel **HG** showed the corresponding acid–base responsiveness. As shown in Fig. 2, after the addition of several drops of the CH_3COOH solution, intermolecular hydrogen bonds have been destroyed.[20] Correspondingly, the supramolecular hydrogel dissociated into a transparent solution within a short time. The fiber-like structure was clearly observed by scanning electron microscopy (Fig. S18a, ESI†). In the ^1H NMR spectrum (Fig. S19, ESI†), H_1, H_2, H_3 and H_4 signals of **BTAP5** showed a gradual downfield shift. This results also suggested that intermolecular hydrogen bonds are destroyed. Subsequent addition of NaOH aqueous solution to the transparent solution led to the recovery of gel state.

Inspired by the applications of dynamic characteristics of ion competitive coordination in the area of self-organization and supramolecular transformations,[21] the anion-stimuli-responsive behavior of the resultant supramolecular hydrogels was expected. As shown in Fig. 2, if ClO_4^- was added to the viscous solution at high temperature, the obtained solution could not form a supramolecular gel on cooling, and the viscous solution ultimately became a turbid solution. As detected by SEM measurement (Fig. S18b, ESI†), the sheet-like structure of hydrogel was also destroyed and turned into a block microstructure after the addition of $KClO_4$. ^1H NMR investigation of **BTAP5** (Fig. S20, ESI†) evidenced that this stimuli-responsive gel–sol phase transition was essentially a consequence of the ClO_4^--induced disassembly. The possible cause of this stimulus response is that ClO_4^- have a stronger binding capacity than cavity of pillararene with *n*-butyltrimethyl ammonium.

In addition, if the competitive guest adiponitrile was added to the viscous solution at high temperature, the obtained
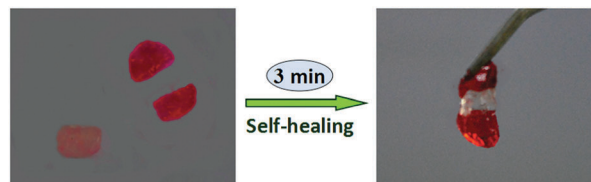
solution could not form a supramolecular hydrogel on cooling due to adiponitrile having stronger competitive binding with pillar[5]arenes than the *n*-butyltrimethyl ammonium,[22] resulting in destroying the [c2]daisy chain dimers (Fig. 2). The SEM measurement (Fig. S18c, ESI†) also showed the sheet structure of hydrogel were destroyed and turned into a interweaved network structure after the addition of adiponitrile.

Owing to dynamic reversibility of hydrogen bonding interactions and π–π stacking interactions, the self-healing property of the supramolecular hydrogel **HG** was studied. As depicted in Fig. 3, three pieces of hydrogels were prepared, of which two hydrogel pieces were colored with a methyl red dye to render a better contrast, and the other is colorless. Interestingly, three pieces of hydrogel are put together, and they can merge into a single one autonomously in 3 min, and the joint is strong enough to be lifted without breakage of the three parts. After 24 h, it was found that the color pink gradually spread into the colorless part, which again verified the self-healing behavior. It is worth to notice that the healing process in the supramolecular **HG** hydrogel is automatically without external treatment, which is advantageous comparing with the materials that needs external intervention to heal cracks.

Next, the cation sensing ability of this supramolecular hydrogel was also investigated. The recognition profiles of hydrogel (5 wt%) toward various cations, including Fe^{3+}, Na^+, Mg^{2+}, Ba^{2+}, Al^{3+}, Ca^{2+}, Ni^{2+}, Zn^{2+}, Mn^{2+}, Co^{2+} and Cr^{3+}, were primarily investigated using fluorescence spectroscopy. As shown in Fig. S21 (ESI†), when adding one equivalent of Fe^{3+} to the supramolecular hydrogel **HG**, the fluorescence emission band at 449 nm disappeared. Other cations could not induce similar fluorescence changes (Fig. 4a). Therefore, this hydrogel could effectively sense Fe^{3+} with specific selectivity. Moreover, when gradually adding Fe^{3+}, the emission intensity at 449 nm decreased with the increasing concentration of Fe^{3+} as shown in Fig. 4b. The detection limit of the fluorescence spectral change was calculated on the basis of 7.86×10^{-10} M (Fig. S22, ESI†), indicating the ultra-sensitivity to Fe^{3+}. Compared with other detection techniques and pillararene-based sensors described in previous reports (Tables S1 and S2, ESI†), this work showed a lower detection limit. Therefore, this supramolecular hydrogel with specific response to Fe^{3+} ions has great potential in future biological and environmental monitoring. In addition, Fe^{3+} responsive films based on this supramolecular hydrogel were prepared by pouring the heated water solution of the hydrogel onto a clean glass surface and then drying it in air. These thin films were utilized to sense Fe^{3+}. As shown in Fig. S23 (ESI†), when Fe^{3+} ions were added onto

This journal is © The Royal Society of Chemistry and the Chinese Chemical Society 2018

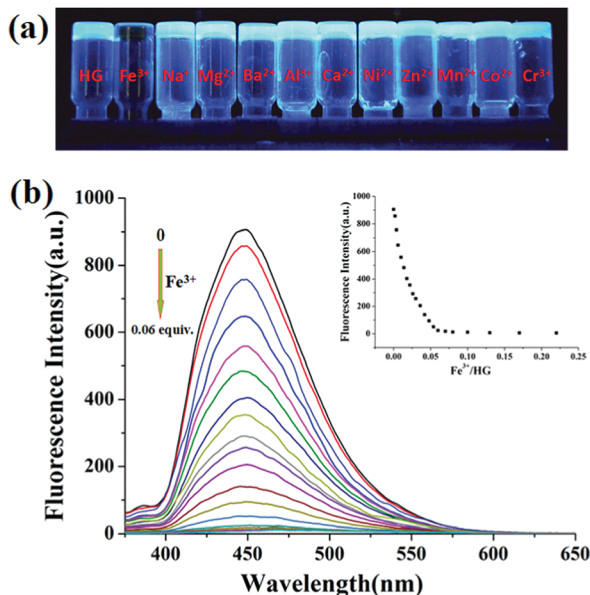*Mater. Chem. Front.*, 2018, **2**, 999–1003 | **1001**

Fig. 4 (a) Photographs of hydrogel **HG** in the presence of 1 equiv. of various cations (using their chlorides as the sources) under UV light. (b) Fluorescence spectra of **HG** (in the gelated state) with increasing concentration of Fe^{3+} (λ_{ex} = 360 nm). Inset: A plot of emission at 449 nm *versus* number of equivalents of Fe^{3+}.
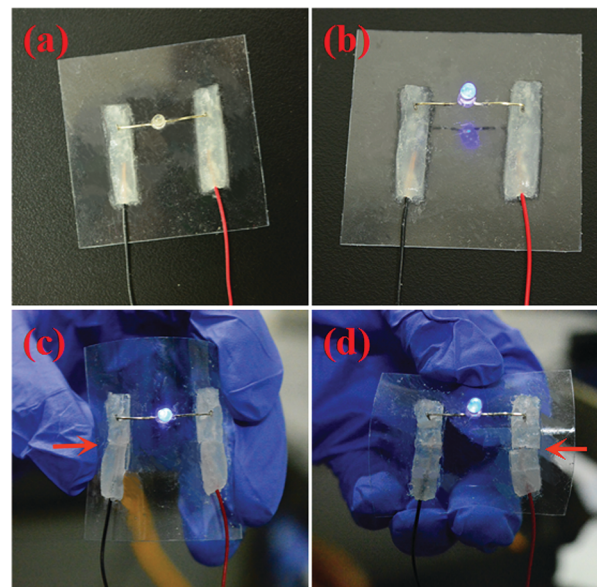

Fig. 5 Self-healing circuit based on hydrogel **HG**: (a and b) optical images of circuit based on **HG** hydrogel film at open and closed states; (c and d) the circuit functions well under bended and fractured states.

the thin film, an obvious color change was observed under irradiation at 365 nm using a UV lamp. Therefore, the thin film could be a convenient test kit for detecting Fe^{3+}. In the FT-IR spectra (Fig. S24, ESI†) and the powder XRD patterns (Fig. S25, ESI†), when Fe^{3+} cations were added to the hydrogel **HG**, all the peaks did not cause obvious shifts. Therefore, we think the heavy atom effect of Fe^{3+} ions causes blue fluorescence quenching.

Finally, conductive properties of the supramolecular hydrogel **HG** have been studied. Because gelator **BTAP5** is a typical cationic pillar[5]arene, there are free-moving charged ions (Br^-) in water solution. Therefore, we believe that this hydrogel has the corresponding conductivity. In order to demonstrate the conductivity of the hydrogel **HG**, we designed a complete circuit composed of a LED bulb with driving voltage of 1.5 V as the electrical load, **HG** hydrogel film as the conductor and one dry batteries (1.5 V) as the power source. As shown in Fig. 5, a circle of **HG** hydrogel thin film was coated on PDMS substrate, then the LED bulb was involved and the power source was linked into the circuit by two copper wires. The bulb was successfully lighted when the circuit was switched to close status, indicating the good conductivity of our hydrogel **HG**. Notably, this circuit could work well under bended, even folded states. At last, the self-healing property of the hydrogel **HG** was also demonstrated on the circuit. As shown in Fig. 5c and d, in a typical test of **HG** hydrogel film was cut and the circuit then became open and the bulb was extinguished. After about 10 s, the circuit was re-established and the LED bulb could be lighted up again. This self-healing test was successfully conducted for multiple times at the same position and also at other positions. Furthermore, the conductivity of **HG** hydrogel film was tested by using four-probe method and can reach as high as 5.7 S m^{-1}. These data and phenomena show the great potential of the hydrogel **HG** for practical applications such as self-healing electronics, biosensors, and artificial skins.

Conclusions

In summary, a functionalized pillar[5]arene-based gelator **BTAP5** has been synthesized, which could further self-assemble into a [c2]daisy chain dimer *via* the intermolecular hydrogen bonding interactions. Furthermore, the [c2]daisy chain dimer could self-assemble to form a fluorescent supramolecular hydrogel (**HG**) at high concentration by the π–π stacking interactions. Interestingly, the obtained supramolecular hydrogel **HG** exhibited thermoreversible gel–sol transformation, whereas, adding the acid (CH_3COOH) resulted in the gel state dissociated into a transparent solution. More importantly, when $KClO_4$ was added to the viscous solution at high temperature, the obtained solution could not form a supramolecular hydrogel on cooling, and the viscous solution ultimately became a turbid solution. Moreover, the supramolecular hydrogel also exhibited competitive agent-responsiveness. These phenomena showed that this supramolecular hydrogel has excellent stimulus-response behavior. When Fe^{3+} are added to the supramolecular hydrogel, the strong blue fluorescence of hydrogel is clearly quenched, and this hydrogel could highly selectively and ultra-sensitively (7.86×10^{-10} M) detect Fe^{3+} cations. Moreover, a thin film of the fluorescent supramolecular hydrogel was prepared, which was confirmed to be a convenient test kit for detecting Fe^{3+}. It is noteworthy that this supramolecular hydrogel is also an excellent self-healing and conductive material. This research not only developed a novel multiple-stimuli responsive supramolecular hydrogels based on pillararene but also expanded the property of pillararene-based gels about self-healing and conductivity.

1002 | *Mater. Chem. Front.*, 2018, **2**, 999–1003

This journal is © The Royal Society of Chemistry and the Chinese Chemical Society 2018

Thus, this good example might stimulate wide interest of scientists for further development of new pillararene-based supramolecular hydrogels.

Conflicts of interest

There are no conflicts to declare.

Acknowledgements

Notes and references

1 (a) L. A. Estroff and A. D. Hamilton, *Chem. Rev.*, 2004, **104**, 1201; (b) N. M. Sangeetha and U. Maitra, *Chem. Soc. Rev.*, 2005, **34**, 821; (c) Y. Gao, F. Zhao, Q. Wang, Y. Zhang and B. Xu, *Chem. Soc. Rev.*, 2010, **39**, 3425; (d) F. Zhao, M. L. Ma and B. Xu, *Chem. Soc. Rev.*, 2009, **38**, 883.

2 O. Wichterle and D. Lim, *Nature*, 1960, **185**, 117.

3 (a) H. Zhang, L. Bré, T. Zhao, B. Newland, M. Da Costa and W. Wang, *J. Mater. Chem. B*, 2014, **2**, 4067; (b) Y. Dong, W. U. Hassan, R. Kennedy, U. Greiser, A. Pandit, Y. Garcia and W. Wang, *Acta Biomater.*, 2014, **10**, 2076.

4 J. Li, *NPG Asia Mater.*, 2010, **2**, 112.

5 (a) T. Aida, E. W. Meijer and S. I. Stupp, *Science*, 2012, **335**, 813; (b) X. Yan, F. Wang, B. Zheng and F. Huang, *Chem. Soc. Rev.*, 2012, **41**, 6042; (c) R. Dong, Y. Zhou and X. Zhu, *Acc. Chem. Res.*, 2014, **47**, 2006.

6 (a) S. S. Babu, V. K. Praveen and A. Ajayaghosh, *Chem. Rev.*, 2014, **114**, 1973; (b) E. A. Appel, J. del Barrio, X. J. Loh and O. A. Scherman, *Chem. Soc. Rev.*, 2012, **41**, 6195.

7 (a) M. Ikeda, T. Tanida, T. Yoshii, K. Kurotani, S. Onogi, K. Urayama and I. Hamachi, *Nat. Chem.*, 2014, **6**, 511; (b) T. Yoshii, M. Ikeda and I. Hamachi, *Angew. Chem., Int. Ed.*, 2014, **53**, 7264; (c) J. Zhou, X. Du, Y. Gao, J. Shi and B. Xu, *J. Am. Chem. Soc.*, 2014, **136**, 2970; (d) L. E. R. O'Leary, J. A. Fallas, E. L. Bakota, M. K. Kang and J. D. Hartgerink, *Nat. Chem.*, 2011, **3**, 821.

8 (a) E. A. Appel, X. J. Loh, S. T. Jones, F. Biedermann, C. A. Dreiss and O. A. Scherman, *J. Am. Chem. Soc.*, 2012, **134**, 11767; (b) H. Komatsu, S. Matsumoto, S.-i. Tamaru, K. Kaneko, M. Ikeda and I. Hamachi, *J. Am. Chem. Soc.*, 2009, **131**, 5580.

9 (a) T. Ogoshi, T. Yamagishi and Y. Nakamoto, *Chem. Rev.*, 2016, **116**, 7937; (b) M. Xue, Y. Yang, X. Chi, Z. Zhang and F. Huang, *Acc. Chem. Res.*, 2012, **45**, 1294; (c) D. Cao, Y. Kou, J. Liang, Z. Chen, L. Wang and H. Meier, *Angew. Chem., Int. Ed.*, 2009, **48**, 9721.

10 (a) J.-F. Chen, Q. Lin, Y.-M. Zhang, H. Yao and T.-B. Wei, *Chem. Commun.*, 2017, **53**, 13296; (b) M. Bojtár, J. Kozma, Z. Szakács, D. Hessz, M. Kubinyi and I. Bitter, *Sens. Actuators, B*, 2017, **248**, 305.

11 C. Sathiyajith, R. R. Shaikh, Q. Han, Y. Zhang, K. Meguellati and Y.-W. Yang, *Chem. Commun.*, 2017, **53**, 677.

12 R. Wang, Y. Sun, F. Zhang, M. Song, D. Tian and H. Li, *Angew. Chem.*, 2017, **129**, 5378.

13 L.-L. Tan, H. Li, Y. Tao, S. X.-A. Zhang, B. Wang and Y.-W. Yang, *Adv. Mater.*, 2014, **26**, 7027.

14 (a) K. Yang, Y. Pei, J. Wen and Z. Pei, *Chem. Commun.*, 2016, **52**, 9316; (b) L.-L. Tan and Y.-W. Yang, *J. Inclusion. Phenom.*, 2015, **81**, 13; (c) Y. Wang, G. Ping and C. Li, *Chem. Commun.*, 2016, **52**, 9858; (d) C. Li, *Chem. Commun.*, 2014, **50**, 12420.

15 (a) L. Liu, D. Cao, Y. Jin, H. Tao, Y. Kou and H. Meier, *Org. Biomol. Chem.*, 2011, **9**, 7007; (b) W. Cui, H. Tang, L. Xu, L. Wang, H. Meier and D. Cao, *Macromol. Rapid Commun.*, 2017, **38**, 1700161; (c) X. Wu, Y. Yu, L. Gao, X.-Y. Hu and L. Wang, *Org. Chem. Front.*, 2016, **3**, 966; (d) P. Chen, J. H. Mondal, Y. Zhou, H. Zhu and B. Shi, *Polym. Chem.*, 2016, **7**, 5221; (e) Y. Yao, Y. Sun, H. Yu, W. Chen, H. Dai and Y. Shi, *Dalton Trans.*, 2017, **46**, 16802.

16 (a) M. Ni, N. Zhang, W. Xia, X. Wu, C. Yao, X. Liu, X.-Y. Hu, C. Lin and L. Wang, *J. Am. Chem. Soc.*, 2016, **138**, 6643; (b) H. Ju, F. Zhu, H. Xing, Z. L. Wu and F. Huang, *Macromol. Rapid Commun.*, 2017, **38**, 1700232.

17 (a) T.-B. Wei, J.-F. Chen, X.-B. Cheng, H. Li, B.-B. Han, Y. Yao, Y.-M. Zhang and Q. Lin, *Polym. Chem.*, 2017, **8**, 2005; (b) Q. Lin, K.-P. Zhong, J.-H. Zhu, L. Ding, J.-X. Su, H. Yao, T.-B. Wei and Y.-M. Zhang, *Macromolecules*, 2017, **50**, 7863; (c) Q. Lin, Y.-Q. Fan, P.-P. Mao, L. Liu, J. Liu, Y.-M. Zhang, H. Yao and T.-B. Wei, *Chem. – Eur. J.*, 2018, **24**, 777.

18 T.-B. Wei, J.-F. Chen, X.-B. Cheng, H. Li, B.-B. Han, Y.-M. Zhang, Y. Yao and Q. Lin, *Org. Chem. Front.*, 2017, **4**, 210.

19 B. Shi, D. Xia and Y. Yao, *Chem. Commun.*, 2014, **50**, 1393.

20 L. Fang, Y. Hu, Q. Li, S. Xu, M. K. Dhinakarank, W. Gong and G. Ning, *Org. Biomol. Chem.*, 2016, **14**, 4039.

21 (a) C. Han, G. Yu, B. Zheng and F. Huang, *Org. Lett.*, 2012, **14**, 1712; (b) S. Sun, X.-Y. Hu, D. Chen, J. Shi, Y. Dong, C. Lin, Y. Pan and L. Wang, *Polym. Chem.*, 2013, **4**, 2224; (c) Q. Lin, T.-T. Lu, X. Zhu, T.-B. Wei, H. Li and Y.-M. Zhang, *Chem. Sci.*, 2016, **7**, 5341.

22 (a) X. Shu, S. Chen, J. Li, Z. Chen, L. Weng, X. Jia and C. Li, *Chem. Commun.*, 2012, **48**, 2967; (b) X. Shu, W. Chen, D. Hou, Q. Meng, R. Zheng and C. Li, *Chem. Commun.*, 2014, **50**, 4820.

This journal is © The Royal Society of Chemistry and the Chinese Chemical Society 2018

Mater. Chem. Front., 2018, **2**, 999–1003 | **1003**